International Journal of Modern Physics E

Investigating the CME in isobaric ($^{96}_{44}$Ru+$^{96}_{44}$Ru and $^{96}_{40}$Zr+$^{96}_{40}$Zr) collisions at $\sqrt{s_{\mathrm{NN}}}$ = 200 GeV using Sliding Dumbbell Method with the STAR detector at RHIC

Jagbir Singh (for the STAR Collaboration) *

Instituto de Alta Investigación, Universidad de Tarapacá, Casilla 7D, Arica, 1000000, Chile
jsingh2@bnl.gov

Received Day Month Year
Revised Day Month Year

The chiral imbalance, coupled with the presence of a strong magnetic field produced during heavy-ion collisions, can result in charge separation along the magnetic field axis, a phenomenon known as the Chiral Magnetic Effect (CME). A novel technique, the Sliding Dumbbell Method (SDM) has been developed to investigate the CME with the RHIC's isobar program. The SDM facilitates the selection of events corresponding to various charge separations (f_{DbCS}) across the dumbbell. A partitioning of the charge separation distributions for each collision centrality into ten percentile bins is done in order to find potential CME-like events corresponding to the highest charge separation across the dumbbell. The study reports the results on CME sensitive γ-correlator ($\gamma = \langle \cos(\phi_a + \phi_b - 2\Psi_{RP}) \rangle$) and δ-correlator ($\delta = \langle \cos(\phi_a - \phi_b) \rangle$) for each bin of f_{DbCS} in each collision centrality for isobaric collisions (Ru+Ru and Zr+Zr) at $\sqrt{s_{\mathrm{NN}}}$ = 200 GeV measured with the STAR detector. Furthermore, the background scaled ratio ($\Delta\gamma_{Ru/Zr}/\Delta\gamma_{Bkg}$) is presented to check for the expected enhancement of the CME in Ru+Ru collisions as compared to Zr+Zr collisions.

Keywords: Quark-Gluon plasma; chiral magnetic effect; heavy-ion collisions; multi-particle correlations; Q-cumulant.

1. Introduction

Quantum Chromodynamics (QCD) predicts the existence of metastable domains characterized by fluctuating topological charges, which can induce chirality imbalance in quarks under extreme conditions of temperature and/or density, such as those present during the formation of the quark-gluon plasma (QGP).[1,2] In non-central heavy-ion collisions, P-odd meta-stable states and the strong magnetic field generated by highly energetic spectator protons leads to the separation of oppositely charged particles along the magnetic field direction and perpendicular to the reaction plane, known as the Chiral Magnetic Effect (CME).[3–6] The CME is under active theoretical[7–10] and experimental[11–15] investigation in relativistic heavy-ion

*J. Singh (for the STAR Collaboration)

collisions, particularly at the Relativistic Heavy Ion Collider (RHIC) and the Large Hadron Collider (LHC).

Isobaric collisions of $^{96}_{44}$Ru+$^{96}_{44}$Ru and $^{96}_{40}$Zr+$^{96}_{40}$Zr nuclei were proposed as a promising approach to address the challenges associated with the detection of the CME in heavy-ion collisions.[16,17] The STAR experiment at RHIC collected data in 2018 on $Ru + Ru$ and $Zr + Zr$ collisions at $\sqrt{s_{\rm NN}} = 200$ GeV to search for the CME in isobaric collision systems.[17] The larger atomic number of Ruthenium ($^{96}_{44}$Ru) compared to Zirconium ($^{96}_{40}$Zr) leads to an increase of approximately 15% in the squared magnetic field in Ru+Ru collisions. This enhanced magnetic field is expected to give rise to a proportional increase in the CME contribution in Ru+Ru collisions, while the similarity in mass numbers in both isobars ensures comparable flow-driven backgrounds. After rigorous data analysis and examination of various CME-sensitive observables, no significant enhancement of the CME signal was found in Ru+Ru collisions compared to Zr+Zr collisions, within uncertainties.[18]

The most commonly used observable in the search for the Chiral Magnetic Effect (CME) is the three particle γ-correlator, initially proposed by Voloshin.[3] It is defined as:

$$\begin{aligned} \gamma_{a,b} = \langle \cos(\phi_a + \phi_b - 2\Psi_{RP}) \rangle &\approx \frac{\langle \cos(\phi_a + \phi_b - 2\phi_c) \rangle}{v_{2,c}} \\ &= \langle \cos(\Delta\phi_a)\cos(\Delta\phi_b) \rangle - \langle \sin(\Delta\phi_a)\sin(\Delta\phi_b) \rangle \end{aligned} \tag{1}$$

where, ϕ_a and ϕ_b denote the azimuthal angles of particles "a" and "b", respectively, while Ψ_{RP} represents the reaction plane angle. $v_{2,c}$ is the elliptic flow of third particle "c" having azimuthal angle ϕ_c. $\Delta\phi_a$ and $\Delta\phi_b$ represent the azimuthal angles of particles "a" and "b" measured with respect to the reaction plane. To estimate v_2 and compute 2- and 3-particle correlators, the Q-cumulant technique[19] is used.

The reaction plane independent 2-particle δ-correlator is also used, which is as follows:

$$\delta_{a,b} = \langle cos(\phi_a - \phi_b) \rangle = \langle cos(\Delta\phi_a)cos(\Delta\phi_b) \rangle + \langle sin(\Delta\phi_a)sin(\Delta\phi_b) \rangle \tag{2}$$

From equations (1) and (2), one can determine in-plane ($\langle cos(\Delta\phi_a)cos(\Delta\phi_b) \rangle$) and out-of-plane ($\langle sin(\Delta\phi_a)sin(\Delta\phi_b) \rangle$) correlations to study the preferential emission of charged particles.

In this study, the Sliding Dumbbell Method (SDM)[20–22] is utilized to identify potential CME-like events. These events are subsequently analyzed using the γ and δ correlators to verify whether or not they exhibit the expected characteristics of CME events.

2. Sliding Dumbbell Method

The "Sliding Dumbbell Method"[20–22] has been designed to identify potential CME-like events in heavy-ion collisions that display higher back-to-back charge separation

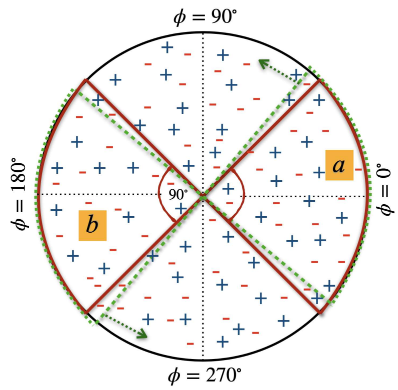

Fig. 1. (Color online) A graphical representation of the transverse (azimuthal) plane showing positive (+) and negative (-) particle hits in an event.

on an event-by-event basis. In the SDM, the azimuthal plane of each event is scanned by sliding a dumbbell-shaped region of $\Delta\phi = 90^\circ$ in steps of $\delta\phi = 1^\circ$ as shown in Fig. 1. This approach helps in identifying the region exhibiting the highest back-to-back charge separation. To quantify this separation, the parameter Db_{+-} is calculated. It represents the sum of the positive charge fraction on one side ("a") of the dumbbell and the negative charge fraction on the opposite side ("b") for each orientation of the dumbbell across the azimuthal plane, is obtained as:

$$Db_{+-} = \frac{n_+^a}{(n_+^a + n_-^a)} + \frac{n_-^b}{(n_+^b + n_-^b)}, \tag{3}$$

where, $n_a^+(n_b^+)$ and $n_a^-(n_b^-)$ represent the number of positive and negative charged particles on sides "a" and "b" of the dumbbell, respectively. The $Db_{+-} = 2$ corresponds to 100% back-to-back charge separation while $Db_{+-} = 1$ means no back-to-back charge separation. Furthermore, the charge excess asymmetry across the dumbbell, Db_{asy}, is defined as:

$$Db_{+-}^{asy} = \frac{(n_a^+ - n_a^-) - (n_b^- - n_b^+)}{(n_a^+ - n_a^-) + (n_b^- - n_b^+)} \tag{4}$$

Here, $n_a^+ - n_a^-$ represents the excess positive charge on the "a" side of the dumbbell, while $n_b^- - n_b^+$ denotes the excess negative charge on the "b" side. By sliding the dumbbell in steps of $\delta\phi = 1^\circ$ across the azimuthal plane, 360 values of both Db_{+-} and Db_{asy} are obtained. The maximum value of Db_{+-}, denoted as Db_{+-}^{max}, is then selected under the constraint $\mid Db_{asy} \mid < 0.25$, ensuring the identification of CME-like events with balanced charge excess asymmetry. The charge separation across the dumbbell, f_{DbCS}, referred to as charge separation, defined as:

$$f_{DbCS} = Db_{+-}^{max} - 1 \tag{5}$$

The charge separation (f_{DbCS}) distributions are obtained for each centrality class for data as well as charge shuffle background (as discussed in section 2.1). These distributions are subdivided into ten percentile bins, ranging from 0-10% (highest charge separation) to 90-100% (lowest charge separation) for each collision centrality. Two (δ) and three particle (γ) correlators are computed for different charge combinations and for each f_{DbCS} bin in each centrality for both data and background.

2.1. *Background Estimation*

We estimate the background contributions to the γ-correlator across different f_{DbCS} percentile bins using the SDM, we account for contributions that may result in higher charge separation purely by statistical fluctuations while preserving the intrinsic particle correlations. This is achieved by randomly shuffling the charges of particles within each event while keeping their momenta (i.e., θ and ϕ) unchanged. The charge-shuffled sample for a given centrality is then analyzed in the same manner as the original dataset.[20] The γ-correlator obtained from this charge-shuffled sample in a particular f_{DbCS} bin is denoted as γ_{ChS}.

Conversely, the charge correlations disrupted by the shuffling process are recovered from the original events corresponding to the same f_{DbCS} bins and the resulting γ-correlator is referred to as γ_{Corr}. Consequently, the total background contribution to the γ-correlator is calculated as:

$$\gamma_{Bkg} = \gamma_{ChS} + \gamma_{Corr} \tag{6}$$

2.2. *Data Analyzed*

We used the minimum bias events from the isobar collisions (${}^{96}_{44}$Ru+${}^{96}_{44}$Ru and ${}^{96}_{40}$Zr+${}^{96}_{40}$Zr) at $\sqrt{s_{\mathrm{NN}}} = 200$ GeV. Events with -35 $< V_z <$ 25 cm and tracks with $|\ \eta\ | < 1$, $0.2 < p_T < 2.0$ GeV/c and DCA $<$ 3 cm are used for the analysis. After all event selection cuts, we analyze approximately 1.7 billion minimum-bias (MB) events each for Ru+Ru and Zr+Zr collisions.

3. Results and Discussions

The f_{DbCS} distributions for Ru+Ru and Zr+Zr collisions are compared in Fig. 2 for different collision centralities. It is observed that f_{DbCS}^{Ru+Ru} distributions are almost similar to f_{DbCS}^{Zr+Zr} distributions. Additionally, these distributions shift toward higher values of f_{DbCS} as the collision centrality decreases.

The dependence of γ-correlator (left) and δ-correlator (right) on f_{DbCS} is displayed in Fig. 3 for opposite-sign and same-sign charge pairs for 0-60% collision centrality for Ru+Ru (blue color) and Zr+Zr (red color) collisions at $\sqrt{s_{\mathrm{NN}}} = 200$ GeV. It is observed that $\gamma_{OS} > 0$ and $\gamma_{SS} < 0$ for the highest f_{DbCS} bins, specifically 0-20% (0-30%) for 0-40% (40-60%) collision centralities, consistent with expectations

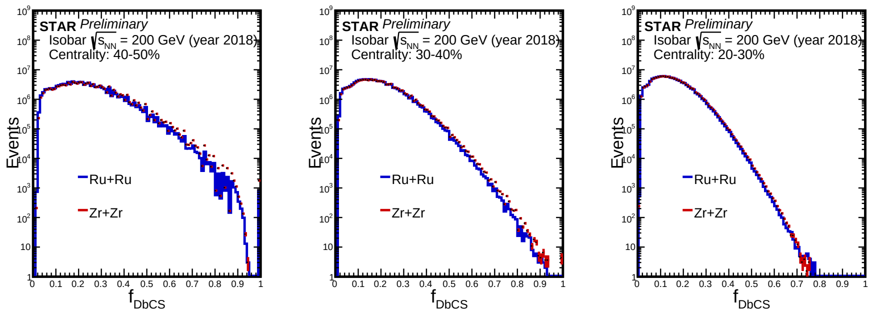

Fig. 2. (Color online) Comparison of f_{DbCS} distributions for Ru+Ru and Zr+Zr collisions at $\sqrt{s_{\rm NN}} = 200$ GeV for different collision centralities.

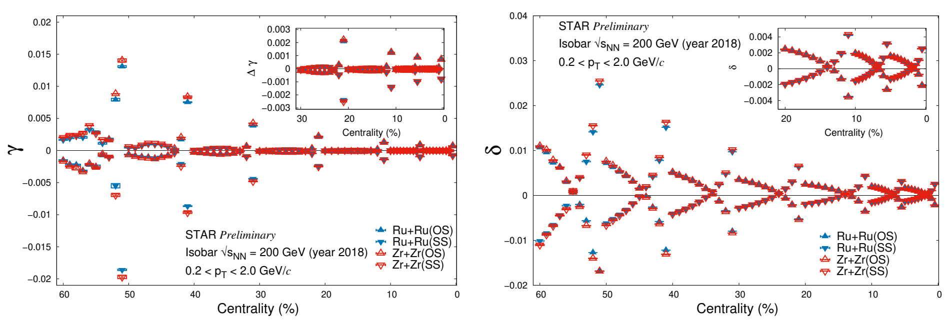

Fig. 3. (Color online) γ (Left) and δ (Right) dependence on f_{DbCS} for 0-60% collision centralities for Ru+Ru and Zr+Zr collisions at $\sqrt{s_{\rm NN}} = 200$ GeV. Boxes represent the systematic errors while the statistical errors (represented by bars) are within the marker sizes.

for CME-like events. Also, $\delta_{SS} > 0$ and $\delta_{OS} < 0$ for the top f_{DbCS} bins, while for lower f_{DbCS} bins, $\delta_{SS} < 0$ and $\delta_{OS} > 0$. Additionally, it is noteworthy that the magnitude of the γ (δ)-correlator is slightly higher for Zr+Zr collisions compared to Ru+Ru collisions.

Figure 4 shows the dependence of in-plane and out-of-plane correlations on f_{DbCS} for opposite-sign (left) and same-sign (right) charge pairs in Ru+Ru and Zr+Zr collisions at $\sqrt{s_{\rm NN}} = 200$ GeV for 0-60% collision centralities. For the top 20% f_{DbCS} bins, out-of-plane correlations are stronger than in-plane correlations for both same-sign and opposite sign charge pairs, suggesting a out-of-plane charge separation.

Figure 5 illustrates the dependence of $\Delta\gamma$ on f_{DbCS} for Ru+Ru (Left) and Zr+Zr (Right) collisions, along with their respective backgrounds i.e., $ChS_{Ru/Zr}$ and $Corr_{Ru/Zr}$, for 0-60% collision centralities. The values of $\Delta\gamma$'s in the top f_{DbCS} bins are enhanced many times than the average values.[18] The data points ($\Delta\gamma_{data}$) for the top 20% f_{DbCS} bins have larger values than the total background contribu-

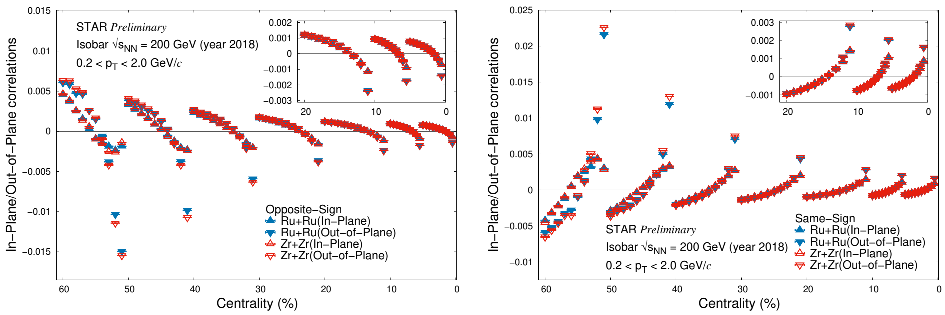

Fig. 4. (Color online) The dependence of in-plane and out-of-plane correlations on f_{DbCS} for 0-60% collision centralities in Ru+Ru and Zr+Zr collisions at $\sqrt{s_{\rm NN}}$ = 200 GeV is shown for opposite-sign (left) and same-sign (right) charge pairs.

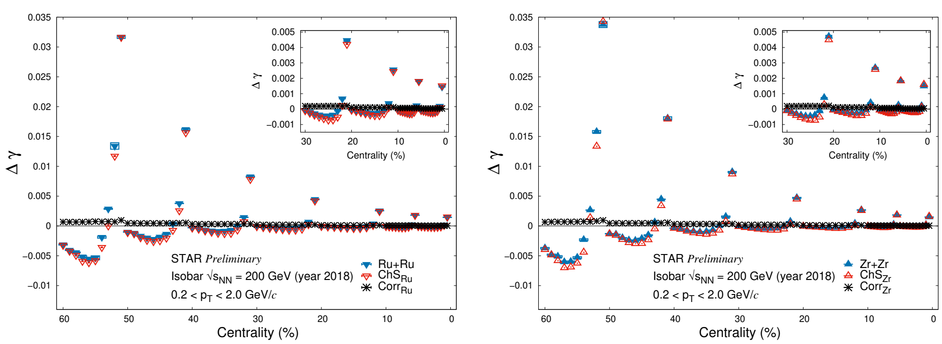

Fig. 5. (Color online) $\Delta\gamma$ dependence on f_{DbCS} for Ru+Ru (Left) and Zr+Zr (Right) collisions, including $ChS_{Ru(Zr)}$ and $Corr_{Ru(Zr)}$ backgrounds for 0-60% collision centralities. The boxes indicate the systematic errors, while the statistical errors, represented by bars, are within the marker sizes.

tion ($\Delta\gamma_{ChS} + \Delta\gamma_{Corr}$) in the 30-50% centrality range.

The ratio $\Delta\gamma_{\rm Data}/\Delta\gamma_{\rm Bkg}$ for Ru+Ru and Zr+Zr collisions for top 20% f_{DbCS} bins is presented for the first time in Fig. 6. It is observed that this ratio exceeds unity by approximately 2-6% for collision centralities within the 10-50% range. The ratios agree within uncertainties for both Ru+Ru and Zr+Zr collisions. No significant enhancement is observed in the background-scaled $\Delta\gamma$ of Ru+Ru relative to Zr+Zr for the top 20% f_{DbCS} bins.

Figure 7 presents the “double ratio”, which compares the $\Delta\gamma_{\rm Data}/\Delta\gamma_{\rm Bkg}$ ratios between Ru+Ru and Zr+Zr collisions for top 20% f_{DbCS} bins. A “Pol0 fit” (straight line fit) was applied to the double ratio, resulting in a fitted value of 1.007 $\pm$ 0.003 for 0-60% centralities. This result suggests no significant enhancement of the CME signal in Ru+Ru collisions relative to Zr+Zr collisions, contrary to the initial expectations for isobar collisions.[18]

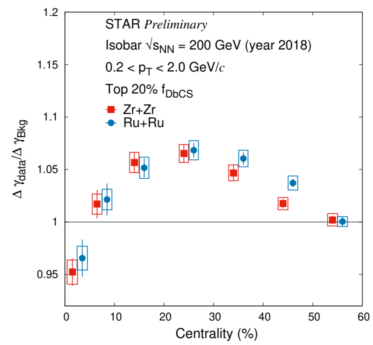

Fig. 6. (Color online) $\Delta\gamma_{Data}/\Delta\gamma_{Bkg}$ for Ru+Ru and Zr+Zr collisions at $\sqrt{s_{\rm NN}}$ = 200 GeV as a function of collision centrality. The statistical errors are represented by bars, while the systematic errors are depicted by boxes.

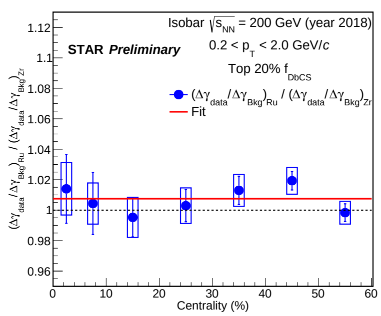

Fig. 7. (Color online) The double ratio $(\frac{(\Delta\gamma_{Data}/\Delta\gamma_{Bkg})_{Ru}}{(\Delta\gamma_{Data}/\Delta\gamma_{Bkg})_{Zr}})$ for 0-60% collision centralities. A straight-line (Pol0) fit is applied to the data, represented by the red line. The statistical errors are represented by bars, while the systematic errors are depicted by boxes.

4. Conclusions

In this study, isobaric collision data was analyzed using the Sliding Dumbbell Method (SDM), which identifies back-to-back charge separation on an event-by-event basis within each collision centrality. The γ and δ correlators exhibited a significant enhancement in the top f_{DbCS} bins compared to the average values across centralities for both same-sign (SS) and opposite-sign (OS) charge pairs. The γ-correlator was found to be positive for OS pairs and negative for SS pairs, while the δ-correlator displayed the opposite trend in top f_{DbCS} bins. Additionally, both SS and OS charge pairs exhibited stronger out-of-plane correlations in the top f_{DbCS} bins, consistent with out-of-plane charge separation, indicating that these bins contain the potential CME-like events. Similar trends were observed in charge-shuffle background but with reduced magnitudes in both isobars. However, the double ratio ($\frac{(\Delta\gamma_{Data}/\Delta\gamma_{Bkg})_{Ru}}{(\Delta\gamma_{Data}/\Delta\gamma_{Bkg})_{Zr}}$) for top 20% f_{DbCS} bins suggests no significant enhancement of the CME signal in Ru+Ru collisions compared to Zr+Zr collisions, contradicting initial expectations for isobaric collisions. In the various techniques studied by the STAR experiment, the anticipated enhancement in Ru+Ru, due to a stronger magnetic field, has not been observed. Further theoretical and experimental investigations are necessary to refine the interpretation of these findings and to develop more robust methodologies for isolating the CME signatures in heavy-ion collisions.

References

1. E. V. Shuryak, *Phys. Lett. B* **78**, 150 (1978).
2. D. Kharzeev, R.D. Pisarski and M.H.G. Tytgat, *Phys. Rev. Lett.* **81**, 512 (1998).
3. S. A. Voloshin, *Phys. Rev. C* **70**, 057901 (2004).
4. D. Kharzeev, *Phys. Lett. B* **633**, 260 (2006).
5. K. Fukushima, D. E. Kharzeev, and H. J. Warringa, *Phys. Rev. D* **78**, 074033 (2008).
6. D. E. Kharzeev, L. D. McLerran, and H. J. Warringa, *Nucl. Phys. A* **803**, 227 (2008).
7. D. Kharzeev, J. Liao, S. Voloshin and G. Wang, *Progress in Particle and Nuclear Physics* **88**, 1 (2016).
8. V. Koch, S. Schlichting, V. Skokov, P. Sorensen, J. Thomas, S. Voloshin et al., *Chinese Physics C* **41**, 072001 (2017).
9. B. Schenke, C. Shen and P. Tribedy, *Phys. Rev. C* **99**, 044908 (2019).
10. J. Zhao and F. Wang, *Progress in Particle and Nuclear Physics* **107**, 200 (2019).
11. B. I. Abelev et al. [STAR collaboration], *Phys. Rev. Lett.* **103**, 251601 (2009).
12. L. Adamczyk et al. [STAR collaboration], *Phys. Rev. C* **88**, 064911 (2013).
13. A. M. Sirunyan et al. [CMS collaboration], *Phys. Rev. C* **97**, 044912 (2018).
14. S. Acharya et al. [ALICE collaboration], *Phys. Lett. B* **777**, 151 (2018).
15. M. S. Abdallah et al. [STAR collaboration], *Phys. Rev. Lett.* **128**, 092301 (2022).
16. S. A. Voloshin, *Phys. Rev. Lett.* **105**, 172301 (2010).
17. V. Koch, et al., *Chin. Phys. C* **41**, 072001 (2017).
18. M. S. Abdallah et al. [STAR Collaboration], *Phys. Rev. C* **105**, 014901 (2022).
19. A Bilandzic, R Snellings and S Voloshin, *Phys. Rev. C* **83**, 044913 (2011).
20. M.M. Aggarwal, A. Attri, S. Parmar, A. Sharma and J. Singh, *Pramana - J. Phys* **98**, 117 (2024).
21. J. Singh (for the STAR Collaboration), *Springer Proc. Phys.* **304**, 464 (2024).
22. Jagbir Singh, Ph.D. Thesis, Panjab University, Chandigarh, INDIA (2024).